THE JOURNAL OF PHYSICAL CHEMISTRY C

Article

pubs.acs.org/JPCC

Ammonia Adsorption and Co-adsorption with Water in HKUST-1: Spectroscopic Evidence for Cooperative Interactions

Nour Nijem,*[,†,‡] Katrin Fürsich,[†,‡] Hendrik Bluhm,[‡] Stephen R. Leone,[†,‡] and Mary K. Gilles[‡]

[†]Departments of Chemistry and Physics, University of California Berkeley, California 94720, United States

[‡]Chemical Sciences Division, Lawrence Berkeley National Lab, 1-Cyclotron Road, Berkeley, California 94720, United States

Supporting Information

ABSTRACT: Ammonia interactions and competition with water at the interface of nanoporous metal organic framework thin films of HKUST-1 (Cu_3Btc_2, Btc = 1,3,5-benzenedicarboxylate) are investigated with ambient pressure X-ray photoelectron spectroscopy (APXPS). In the absence of water, ammonia adsorption at the Cu^{2+} metal center weakens the metal−linker bond of the framework. In the presence of water, due to the higher binding energy (adsorption strength) of ammonia compared to water, ammonia replaces water at the unsaturated Cu^{2+} metal centers. The water molecules remaining in the pores are stabilized by hydrogen bonding to ammonia. Hydrogen bonding between the water and ammonia strengthens the metal−ammonia interaction due to cooperative interactions. Cooperative interactions result in a reduction in the metal center oxidation state facilitating linker replacement by other species explaining the previously reported structure degradation.

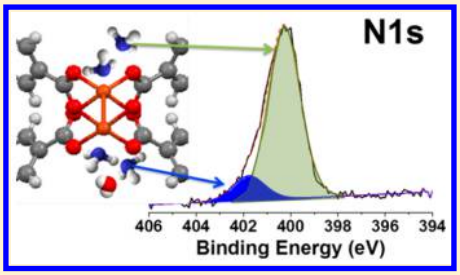

1. INTRODUCTION

Metal organic frameworks (MOFs) are attractive in areas related to gas separation and storage, gas sensing, catalysis, air purification, and removal of toxic gases.[1−10] MOFs are porous materials composed of metal centers, or nodes, connected with organic components to form three-dimensional ordered networks. MOFs exhibit large surface areas, high porosity, and structural tunability by varying the attached linkers and metal nodes to modify the pore chemistry.[11,12] Removal of toxic gases, such as ammonia, by MOFs has been a focus of recent research.[7] HKUST-1 (Cu_3Btc_2) with the open Cu^{2+} metal sites has been investigated for the removal of ammonia, nitric oxide, and CO_2.[13−16] Ammonia uptake in HKUST-1 exceeds that of porous carbon.[13−15] However, the degradation associated with the presence of moisture renders HKUST-1 unsuitable for practical applications.[13−17] Therefore, probing co-adsorption of gases in MOFs with open metal center such as HKUST-1 is important. Previous works characterizing water and ammonia exposure of HKUST-1 were performed ex situ after exposure to high concentrations of water and ammonia. Post-exposure characterization indicated degradation with ammonium ions reacting with the linker, while the copper metal center was hydroxylated.[13−17] Ex situ characterization provides useful information; however, interactions during initial co-adsorption at low pressures can only be revealed through in situ characterization. Probing interactions during co-adsorption of guests is fundamentally important because it simulates conditions similar to those experienced in practical applications, for example, during gas separation. Probing adsorptive interactions in situ with chemical specificity can reveal mechanisms not observed by adsorption isotherms alone.[18−24] Therefore, an in situ study of the co-adsorption is critical for revealing adsorbate−metal center and adsorbate−adsorbate interactions. Here, competitive interactions of water and ammonia are interrogated by the APXPS technique at low relative humidity and partial pressure of ammonia to investigate interactions leading to degradation.

In this work, we report evidence for cooperative interactions between ammonia and water with the Cu^{2+} metal centers of HKUST-1 caused by hydrogen bonding of water with ammonia. The ammonia−Cu^{2+} interaction strength is increased leading to the degradation of the framework observed in previous work.[13]

2. MATERIALS AND METHODS

2.1. Thin Film Synthesis. HKUST-1 thin films (40 layers, ∼100 nm) were synthesized using the layer-by-layer liquid phase epitaxy method on a hydroxylated SiO_2 coated quartz crystal microbalance (QCM) substrate following published methods.[25−27] The SiO_2 coated QCM substrates (QCM crystals with SiO_2 coatings were purchased from Biolin Scientific) were cleaned by dipping them into a 2% sodium dodecyl sulfate followed by deionized water rinse with a final step of UV ozone exposure for 10 min. The UV ozone exposure creates hydroxyl groups on the surface. The film deposition was performed by flowing a 0.2 mM ethanolic solution of copper acetate over the functionalized substrate followed by a solvent rinse (ethanol), then flowing a 1 mM ethanolic solution of trimesic acid, followed by another solvent rinse, for a total of 40 layers (∼100 nm). Deposition temperature was kept at 22 °C,

Received: June 15, 2015
Revised: October 8, 2015
Published: October 9, 2015

DOI: 10.1021/acs.jpcc.5b05716
J. Phys. Chem. C 2015, 119, 24781−24788

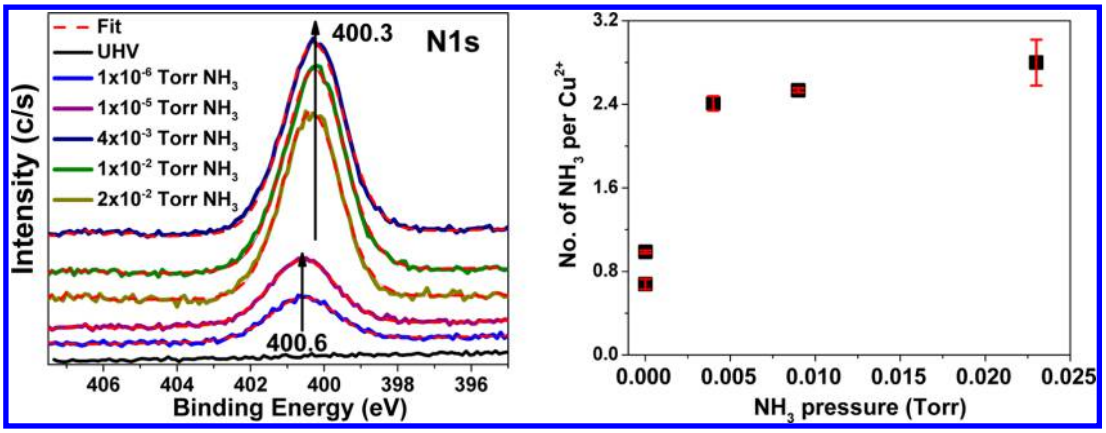

Figure 1. Left: N 1s photoelectron spectra as a function of ammonia pressure. With increasing NH_3 loading, a slight decrease (−0.3 eV) in the N 1s peak binding energy occurs. Right: number of ammonia molecules per copper as a function of ammonia pressure. N 1s and Cu 2p photoelectron spectra are collected at 600 and 1140 eV photon energies, respectively, and the amount adsorbed is calculated from the integrated peak areas measured at equilibrium. The amount of ammonia absorbed increases rapidly and plateaus at ∼0.025 Torr at ∼2.8 ± 0.2 NH_3 per Cu^{2+}. Equilibrium was reached at each pressure, and measurements are performed 10 min after gas introduction.

and the mass deposition per layer was monitored by the QCM technique. Layer thickness is calculated from the density and deposited mass. The X-ray diffraction pattern of a 40 layer HKUST-1 thin film is shown in Figure S1 of the Supporting Information.

2.2. Ambient Pressure X-ray Photoelectron Spectroscopy (APXPS). Synchrotron X-ray spectroscopy measurements in the presence of a gas were performed at the Advanced Light Source (ALS) beamline 11.0.2. The experimental setup is described in detail in a paper by Ogletree et al. and a review by Bluhm et al.[28,29] HKUST-1 thin film samples were heated in situ overnight at a temperature of 110 °C in ultrahigh vacuum (UHV) using a resistive button heater. A photon energy of 490 eV is used for C 1s core electrons, 600 eV for the N 1s core electrons, 735 eV for O 1s, and 1140 eV for Cu 2p; these photon energies result in electrons escaping with energies of 200 eV, providing similar sample probe depths. An additional set of data for each element was collected at 735 eV and used for calibration of binding energy shifts. Cu NEXAFS spectra were collected in partial electron yield mode with a kinetic energy of 750 eV and a kinetic energy bandwidth of 50 eV. The amount of adsorbed gas per copper was calculated from the integrated areas of the photoelectron peaks. The integrated peak area was normalized by the sensitivity factors of the different elements and the photon flux, measured using a calibrated photo diode.[30] Reduction of the metal center oxidation state and framework degradation due to X-ray exposure were previously observed and can be clearly identified in HKUST-1 NEXAFS spectra.[18] To prevent sample degradation, measurements were performed at different sample positions.[18] The uncertainties in the Cu^{1+} percentages are less than 5%, and in the ratios ∼±4% of the values. Peak positions were fixed, and the full width at half-maxima is allowed to vary during the fitting within some constraints leading to a change in the area. Uncertainties were determined by differences in the peak areas when varying the baseline slopes and upper and lower energy limits used to fit the peak areas. The time for dosing the gas into the chamber followed by data acquisition precludes detailed kinetic studies. Performing measurements at lower temperatures would allow higher loadings (higher intensity) to be achieved and possible extraction of kinetic and thermodynamic information. However, kinetic studies may be limited to relatively slow processes due to the time required for data acquisition (∼20−30 s) and time for gas dosing (∼15 s). The integrated areas of the peaks were measured at initial dosing after 1 min and after 4 min, and no change is observed. To ensure equilibrium, we waited 10 min after gas dosing for measurements reported here. Thus, the combined instrumental (beamline + spectrometer) resolution varies from 0.32 eV at 490 eV to 0.43 eV at 1140 eV incident photon energy.

3. RESULTS AND DISCUSSION

3.1. NH_3 Interactions in HKUST-1. To determine the spectroscopic signature of the adsorbed ammonia, ammonia interactions with HKUST-1 were studied as a function of ammonia uptake by X-ray photoelectron spectroscopy (XPS) and NEXAFS. These experiments were performed prior to studying the co-adsorption of ammonia and water in HKUST-1.

Spectroscopic Signature and Loading of Ammonia from APXPS. The left panel of Figure 1 shows the N 1s photoelectron spectra of HKUST-1 as a function of ammonia pressure. At the lowest ammonia pressures (a loading of <∼0.8 NH_3:Cu^{2+}), the N 1s peak at 400.6 eV is attributed to physisorbed ammonia at the Cu^{2+} sites. Changes in color due to adsorption at the Cu^{2+} site have been reported as a result of ammonia adsorbed in HKUST-1 binding to the unsaturated metal centers via Lewis acid−base interactions.[31] With increasing ammonia pressures (>10^{-5} Torr), the N 1s peak shifts by −0.3 eV. This decrease in binding energy with increasing ammonia uptake indicates a slight weakening of the ammonia−Cu^{2+} interaction (less electron donation from ammonia to the metal). This shift does not result from sample charging because different peaks shift differently. A decrease in the heat of adsorption of ammonia with increasing ammonia loading has been attributed to ammonia−ammonia interactions on neighboring Cu^{2+} sites.[16] Intermolecular interactions were previously observed by vibrational spectroscopy and result in a shift of the vibrational frequency of the adsorbed molecules.[32] The right panel of Figure 1 shows the number of ammonia molecules per copper (calculated from the ratios of integrated areas of the N 1s and Cu 2p photoelectron peaks) as a function of ammonia pressure at equilibrium. At a pressure of 0.025 Torr a plateau is reached that corresponds to an occupation of ∼2.8

DOI: 10.1021/acs.jpcc.5b05716
J. Phys. Chem. C 2015, 119, 24781−24788

± 0.2 NH_3 per Cu^{2+}, a value higher than previously reported (~1.5 NH_3:Cu^{2+}).[13,16]

XPS is surface sensitive (inelastic mean free path of electrons is ~1−2 nm under the conditions used in these experiments and probe depth is 3−6 nm) and specifically provides information about the gas porous material interface and chemical interactions. Hence, these measurements differ from adsorption isotherms that average over the entire sample and lack chemical specificity. The amount of adsorbed ammonia per copper at a pressure of 10^{-5} Torr, <~0.8 ± 0.1 NH_3:Cu^{2+}, (calculated from the N 1s peak integrated area) indicates occupation of nearly all metal sites with a saturation of ~2.8 NH_3:Cu^{2+} at 0.023 Torr. Compared to bulk powder MOF measurements, the metal center saturation occurs at a lower ammonia pressure.[15] The higher ammonia adsorption for the 40 layer film indicates a higher local loading at the HKUST-1 thin film surface. The 40 layer HKUST-1 film is oriented in the [222] crystallographic direction with the tetrahedral small pores (~5 Å) aligned parallel to the surface (Figure S1).[18] Adsorption of one ammonia molecule (gas kinetic diameter of 3.57 Å) in these constricted pores could facilitate ammonia−ammonia interactions and result in higher local loading. Moreover, constriction of the pores interconnecting the small tetrahedral pockets to the larger cavities would enhance the adsorbate interaction with the framework walls providing additional adsorption sites. These observations are consistent with a higher loading at the MOF peripheries that occur due to the presence of local minima for adsorption.[32,33]

Changes of the Copper−Ligand Bond with Ammonia Adsorption. To examine changes in the metal−linker bonding and the unsaturated metal center oxidation state, NEXAFS spectra of the Cu L3-edge are recorded before and after ammonia exposure. Figure 2 shows NEXAFS Cu L3-edge

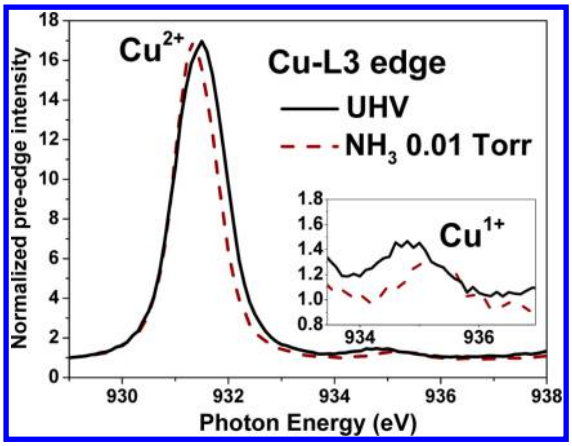

Figure 2. Cu L3-edge NEXAFS spectra under ultrahigh vacuum (UHV) (solid line) and under 0.01 Torr ammonia (dashed spectrum), slight shifts in the Cu^{2+} and Cu^{1+} peaks (discussed in the text) are observed. Inset: Cu^{1+} peak.

spectra under UHV (black solid line) and at 0.01 Torr ammonia (brown dashed line), where the loading is ~2.5 NH_3:Cu^{2+}. The NEXAFS spectra are normalized to the pre-edge intensity. The Cu^{2+} L3 peak at 931.4 eV arises from the electric dipole-allowed 2p−3d transition, and the Cu^{1+} L3 peak arises from $2p^63d^{10}$ to $2p^53d^{10}4s^1$ transition.[34,35]

Using the Cu 2p photoelectron spectra, the Cu^{1+} percentage calculated from the peak intensities is ~3.5% Cu^{1+} (Figure S2 (top) of Supporting Information). This value is consistent with our previous studies on pristine thin films.[36] Cu^{1+} defects in the thin films are attributed to missing linkers and partially coordinated linkers to the copper dimers.[18,36,37] A −0.2 eV shift in the L3 Cu^{2+} peak position indicates a decrease in ligand field splitting and a weakening of the ligand−metal bond due to the interaction with ammonia.[38] The L3 Cu^{2+} peak position is a measure of the 2p−3d transitions in the metal. The ligand field splitting occurs due to hybridization of the 2p orbitals of the oxygen and the 3d orbitals of the metal causing a splitting in the energy of the metal's 3d orbitals. If the metal−ligand bond weakens, this would alter the hybridization of the p and d orbitals of the copper and the ligand's 2p oxygen (decrease in the metal orbital filling). Therefore, a decrease in the L3 Cu^{2+} peak position indicates a decrease in the energy required for the 2p−3d transition in the metal. This effect is caused by the decrease in 3d metal orbitals splitting (ligand field splitting), a result of the weaker hybridization of the oxygen p orbitals with 3d orbitals of the copper. Hydrogen bonding between the ammonia molecules on neighboring sites and the ligand may contribute to the weakening of the Cu−O bond and stabilization of the second ammonia. The peak line width also decreases by 0.2 eV. The L3 peak of the Cu^{1+} (inset of right panel of Figure 2) shifts toward higher photon energy with adsorption of NH_3 at the Cu^{1+} defects, indicating a change in 4s orbitals. Indeed, interaction of ammonia with materials having Cu^{1+} was previously observed by infrared photodissociation spectroscopy to be electrostatic in nature, which is enhanced by hybridization of the 4s and 3d orbitals of the Cu^{1+}.[39]

3.2. Co-adsorption of NH_3 and H_2O in HKUST-1 Film. *Spectroscopic Signature of NH_3 and Water Co-adsorbed in HKUST-1.* Co-adsorption of water and ammonia in HKUST-1 was investigated by exposing an activated (sample heated at 110 °C in vacuum to remove residual solvent) thin film to water vapor and introducing ammonia thereafter. The left panel of Figure 3 shows O 1s photoelectron spectra of HKUST-1 under UHV (top spectrum), at 0.26 Torr H_2O (middle spectrum), and after addition of 0.03 Torr NH_3 (bottom spectrum). The main O 1s peak at 532 eV is assigned to the C−O bond of the Btc linker. The O 1s peak at 533.7 eV, which only appears in the presence of H_2O, is assigned to physisorbed H_2O at the Cu^{2+} metal sites. Note that upon the addition of water vapor or ammonia, the signal intensity decreases due to scattering of electrons by the gas phase water.[40] The water uptake at 0.26 Torr H_2O corresponds to 1.4 H_2O:Cu^{2+}. This loading indicates the presence of a second water molecule that is hydrogen bonded to the primary water molecule adsorbed at Cu^{2+} (three water molecules per Cu−Cu dimer). With addition of 0.03 Torr NH_3, a +0.6 eV shift in the O 1s peak position of adsorbed water is observed (bottom left panel, Figure 3) indicating a change in the interaction of adsorbed water in HKUST-1. Previously, high binding energy O 1s peak positions, observed beyond a monolayer of water adsorption, were attributed to water hydrogen bonding with other water molecules.[41] Therefore, the 534.3 eV peak in the O 1s spectrum indicates hydrogen bonding of the remaining water to ammonia adsorbed at the Cu^{2+} metal center. The N 1s photoelectron spectrum at 0.26 Torr H_2O and with the subsequent addition of 0.03 Torr NH_3 is shown in the right panel of Figure 3. The N 1s peak at 400.3 eV is assigned to NH_3 adsorbed at Cu^{2+} with a loading of 1.4 ± 0.05 NH_3:Cu^{2+} at an ammonia partial pressure of 0.03 Torr and water vapor pressure of 0.26 Torr. This is a significant decrease in loading compared to that

DOI: 10.1021/acs.jpcc.5b05716
J. Phys. Chem. C 2015, 119, 24781−24788

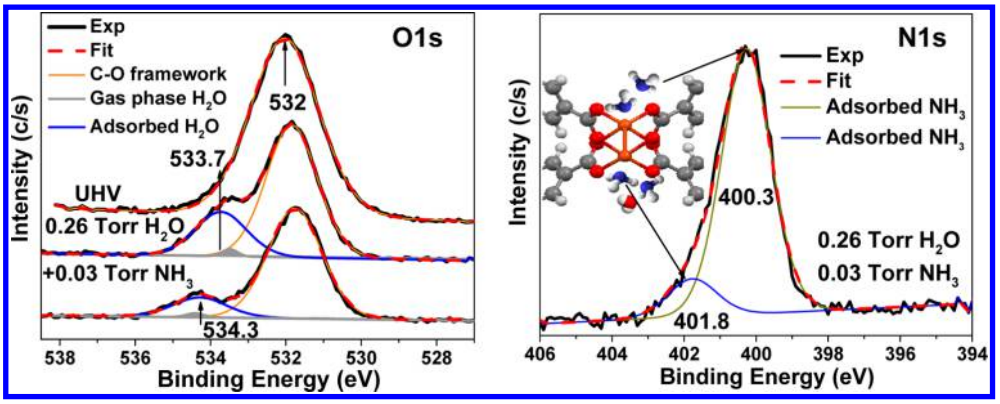

Figure 3. Left: O 1s photoelectron spectra under UHV (top) and 0.26 Torr H_2O (middle), and after addition of 0.03 Torr ammonia (bottom). Right: N 1s photoelectron spectra in the presence of 0.26 Torr H_2O and 0.03 Torr NH_3. The inset is a schematic illustrating the peak assignments. The N 1s peak at 401.8 eV appears only in the presence of water. Water gas phase peaks (gray peaks) shift differently with varying measurement position on the sample due to the inequivalent charging of the gas molecules at the sample surface.

measured in the absence of water (2.8 NH_3:Cu at 0.025 Torr NH_3, see right panel Figure 1), suggesting adsorption of water replacing the second shell ammonia molecules in the larger cages. Comparison of Figure 1 (left) and Figure 3 (right) shows that the shoulder at 401.8 eV in the N 1s photoelectron spectrum only occurs when both water and ammonia are present. This higher binding energy peak position indicates a stronger donation of the nonbonding lone pair electron to the metal due to hydrogen bonding with water. This is consistent with a simplistic initial state model where binding energy peak positions are related to how strongly electrons are bound to the nucleus. Removal of an electron from the nitrogen results in a stronger attraction of the remaining electrons to the nucleus, therefore increasing its binding energy.[18] Changes in the copper metal center due to electron donation from the ammonia to the copper are discussed in the next section.

At a water vapor pressure of 0.26 Torr, at equilibrium the amount of adsorbed ammonia and water molecules per copper as a function of ammonia vapor pressure are summarized in Figure 4. The amount of adsorbed water (calculated from the ratios of integrated areas of the O 1s and Cu 2p photoelectron peaks) drops from 1.4 H_2O:Cu^{2+} to 0.32 H_2O:Cu^{2+} with addition of 0.1 Torr NH_3, indicating replacement of water by ammonia. Ammonia is expected to replace water because of the higher binding energy of ammonia to the Cu^{2+} (~82 kJ/mol) compared to H_2O (~42 kJ/mol).[16,42] Approximately 22 ± 4% of the initial water remains adsorbed in HKUST-1 at 0.1 Torr of ammonia. This is most likely due to stabilization of adsorbed water by hydrogen bonding with ammonia in the larger pores that can fit both adsorbed molecules. The amount of ammonia at the higher binding energy position (401.8 eV) corresponds to ~0.12 NH_3:Cu^{2+} (1 ammonia molecule for every 4 copper dimers).

Changes in Ammonia–Metal Interaction with Coadsorption of Water—Cooperative Interactions. To probe the metal center during co-adsorption of ammonia and water, NEXAFS spectra are recorded before and after exposure to water and ammonia. Figure 5 shows Cu L3-edge NEXAFS spectra under UHV (black line) and after addition of 0.26 Torr H_2O (blue dashed line) and addition of 0.01 Torr NH_3 (brown squares). The Cu^{2+} peak shifts by −0.2 eV with exposure to water, similar

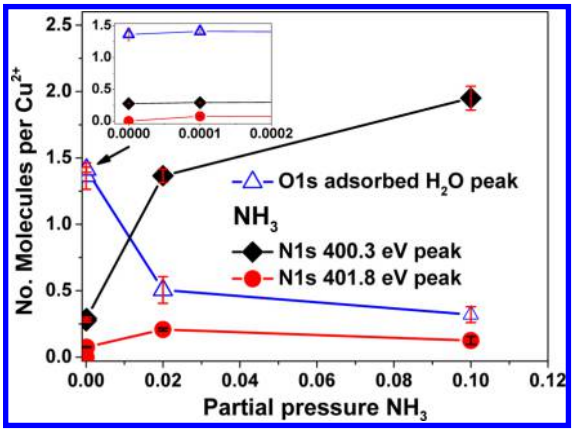

Figure 4. Calculated number of adsorbed water molecules from the O 1s (open triangles) and ammonia N 1s peaks at 400.3 eV (black diamonds) and 401.8 eV (red circles) in the presence of 0.26 Torr of water vapor as a function of ammonia vapor pressure starting from a pressure of 10^{-4} Torr ammonia. As ammonia pressure increases, the preadsorbed H_2O decreases. Measurements are performed after 10 min. Inset: Zoom of data points in the low pressure region.

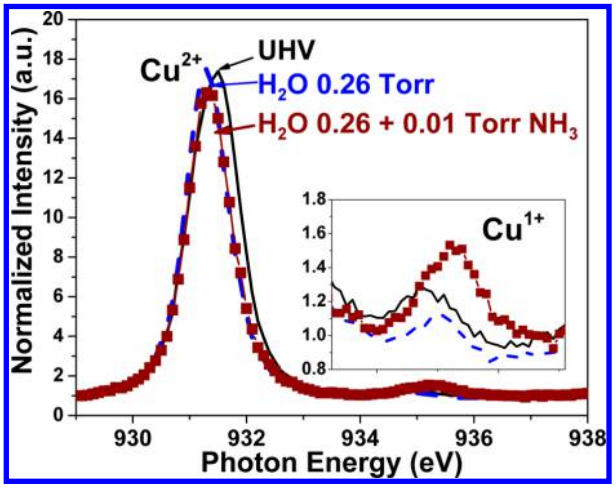

Figure 5. Cu L3-edge NEXAFS spectra of HKUST-1 under ultrahigh vacuum (UHV) (black line) and after exposure to 0.26 Torr water (blue dashed line). The inset shows the Cu^{1+} peak. A −0.2 eV shift in the Cu^{2+} L3 peak position is observed in the presence of water. An increase in the Cu^{1+} peak area is observed in the presence of both water and ammonia.

DOI: 10.1021/acs.jpcc.5b05716
J. Phys. Chem. C 2015, 119, 24781−24788

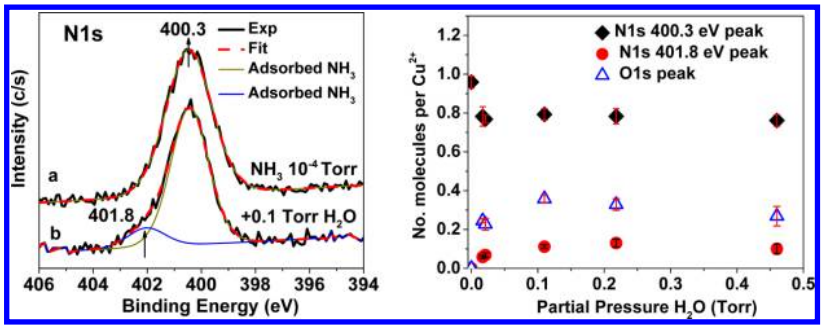

Figure 6. Left: N 1s photoelectron spectra at 10^{-4} Torr ammonia without water vapor (spectrum a) and after addition of 0.1 Torr water vapor (spectrum b). The peak at 401.8 eV only appears when both NH_3 and H_2O are present. Right: Number of molecules of NH_3 (N 1s peaks at 400.3 eV (diamonds) and 401.8 eV (circles)) and H_2O (O 1s peak of adsorbed water at 534.3 eV (triangles)) adsorbed in HKUST-1 as a function of H_2O partial pressure at equilibrium. With the initial addition of water, the adsorbed ammonia decreases due to replacement of adsorbed ammonia (at the second shell) by water. Equilibrium is reached at each pressure by waiting 10 min after introducing the gas.

to what was observed for ammonia (Figure 2, Figure S3) due to an interaction of the lone pair of electrons on the oxygen of the water with the Cu^{2+} in a Lewis base interaction.

As shown in Figure S3, Cu^{2+} L3-edge spectra measured with only water or only NH_3 overlap with one another and are all shifted to lower photon energies than UHV conditions (see Figure 2). In the presence of both water and ammonia, the Cu^{1+} peak is more intense than if only water or only ammonia are present (Figure S3). From the integrated peak areas, the amount of Cu^{1+} from the Cu 2p spectra is ~6% at 0.01 Torr water and 0.26 Torr NH_3. Reduction of the metal center oxidation state indicates that the ammonia adsorbed at the Cu^{2+} acts as a stronger electron donor in the presence of water than in its absence. The change in ammonia interaction with the metal center stems from hydrogen bonding of water and ammonia which polarizes the ammonia molecule and strengthens its electron donation character, an effect referred to as cooperative hydrogen bonding.[43,44] Cooperative hydrogen bonding was previously observed to affect interactions of water bound to metal surfaces.[43,44]

3.3. Cooperative Effect of Ammonia–Ammonia and Ammonia–Water Hydrogen Bonding Interactions. In this section, we compare the interaction of water with preadsorbed ammonia in HKUST-1 at loadings of ~1 NH_3:Cu^{2+} and ~2 NH_3:Cu^{2+}. The objective is to elucidate the influence of ammonia preloading on water incorporation and its effect on the ammonia interaction with the Cu^{2+}.

Initial Loading of ~1 NH_3:Cu^{2+}. The left panel of Figure 6 shows N 1s photoelectron spectra at 10^{-4} Torr ammonia (top spectrum) and after exposure to an additional 0.1 Torr water (bottom spectrum). The ammonia loading of 10^{-4} Torr corresponds to 0.94 NH_3:Cu^{2+}. The right panel of Figure 6 summarizes the number of ammonia and water molecules adsorbed per Cu^{2+} as the partial pressure of water is increased at equilibrium. When 0.1 Torr of water is introduced (corresponding to a loading of 0.35 H_2O:Cu^{2+} (O 1s peak, not shown)), the N 1s peak at 400.3 eV decreases and a second N 1s peak at 401.8 eV appears (Figure 6 left panel). With the addition of water, the integrated areas of the N 1s peaks correspond to loadings of 0.77 NH_3:Cu^{2+} and 0.11 NH_3:Cu^{2+}, respectively (Figure 6 right). Up to ~6% of the adsorbed ammonia is replaced by water (~0.94 NH_3:Cu^{2+} initial loading decreases to 0.88 NH_3:Cu^{2+} after addition of water). This is due to the water increased chemical potential at these pressures as shown by Watanabe et al. allowing replacement of the ammonia adsorbed at the Cu^{2+}.[42] Approximately 12% of the remaining ammonia molecules (0.11 of the total remaining 0.88 NH_3:Cu^{2+}) are hydrogen bonded to water adsorbed at the Cu^{2+} and participate in cooperative interactions (401.8 eV N 1s peak). The next section will contrast the influence of twice the amount of preadsorbed ammonia on promoting water incorporation.

Initial Loading of ~2 NH_3:Cu^{2+}. Figure 7 summarizes the changes in the number of adsorbed molecules starting with

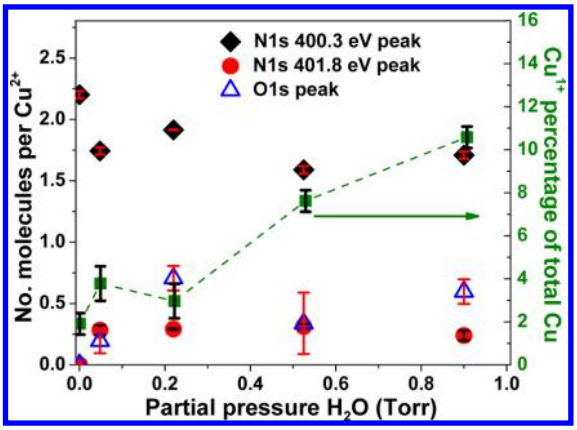

Figure 7. Number of molecules adsorbed as a function of H_2O partial pressure at equilibrium. Values are calculated from the integrated photoelectron peak areas of N 1s (400.3 eV (diamonds) and 401.8 eV (circles)) and the O 1s peak of adsorbed water at 534.3 eV (triangles). In the absence of H_2O, the highest NH_3 loading was ~2.2 ± 0.05 NH_3:Cu^{2+}. The squares represent the calculated percentage of Cu^{1+} as a function of water vapor pressure.

~2.2 NH_3:Cu^{2+} as a function of partial pressure of water. Data are plotted for N 1s (400.3 eV (black diamonds) and 401.8 eV (red circles)) and the O 1s peak of adsorbed water at 534.3 eV (blue open triangles). The percentage of Cu^{1+} (brown squares) is also calculated and increases with water exposure. The slight change in copper oxidation state is caused by an increased donation of electrons from the ammonia to the Cu^{2+} in the presence of water (see section 3.2). After ~0.05 Torr H_2O is added with an initial ammonia loading of 2 NH_3:Cu^{2+} (~0.7 H_2O:Cu^{2+} and ~1.94 NH_3:Cu^{2+}), the intensity of the N 1s and O 1s peaks are relatively independent of the water vapor pressure. Approximately 12% of the total ammonia (a decrease from ~2.2 NH_3:Cu^{2+} to ~1.94 NH_3:Cu^{2+}) is replaced by water at lower binding energy sites (second shell of ammonia). This corresponds to twice as much ammonia replaced by water

DOI: 10.1021/acs.jpcc.5b05716
J. Phys. Chem. C 2015, 119, 24781–24788

compared to the lower ammonia loading conditions. Replacement of the second ammonia is expected because the primary ammonia has a higher binding energy to the Cu^{2+} than water. Cooperative interactions of hydrogen bonded water and the primary ammonia adsorbed at the Cu^{2+} (401.8 eV N 1s peak) result in an increased donation of the nonbonding lone pair electrons of the ammonia to the metal (change in the metal center oxidation state (Figures 5, 7)). The reduced Cu^{1+} increases to ~10% with increasing water loading.

Comparison of the Two Initial Ammonia Loading Conditions. At similar water vapor pressures both the area of the 401.8 eV N 1s peak (~0.24 NH_3:Cu^{2+}) and the amount of adsorbed water (~0.6 H_2O:Cu^{2+}) are a factor of 2 larger at a loading of 2 NH_3:Cu^{2+} than for 1 NH_3:Cu^{2+}.

This higher water uptake and the integrated area of the N 1s 401.8 eV at 2 NH_3:Cu^{2+} suggest an enhancement of water incorporation (due to hydrogen bonding to preadsorbed ammonia) within the pores. Cooperative hydrogen bonding was previously observed to enhance adsorption of ammonia in porous organic polymers.[45] Adsorption of 2 NH_3 molecules per copper promotes hydrogen bonding between the ammonia molecules. Ammonia–ammonia hydrogen bonding makes the second adsorbed ammonia a better proton donor, facilitating hydrogen bonding to water. In the presence of water, and due to hydrogen bonding polarization of the ammonia molecules, an increased electron donation of the primary ammonia to the Cu^{2+} occurs (in a similar fashion to interactions resulting from directly interacting water with primary ammonia).

Two potential sites for water hydrogen bonding to ammonia are schematically shown in Figure 8. Figure 8 is a visualization

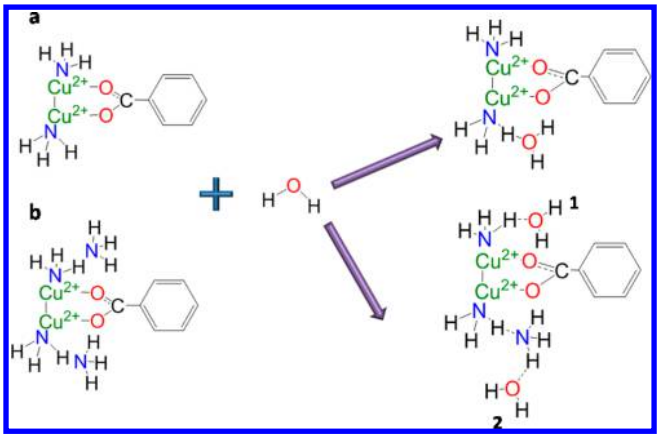

Figure 8. Schematic representation visualizing possible cooperative interactions between water, ammonia, and Cu^{2+} in HKUST 1 for loadings of (a) 1NH_3:Cu^{2+} and (b) 2NH_3:Cu^{2+}. These schematics illustrate possible hydrogen bonding interactions. In case (b), two potential adsorption sites for water are present that could produce the cooperative interactions measured in this work.

of the different adsorption sites present and is not a result of simulations. Water can bind directly to the primary ammonia by replacing the second adsorbed ammonia (second shell ammonia), or water can interact with the secondary adsorbed ammonia molecules. Water adsorption at these two sites could explain the higher 401.8 eV peak area and water incorporation at 2 NH_3:Cu^{2+} compared to lower ammonia loading conditions. The results presented here indicate the need for further theoretical investigations of water and ammonia cooperative interactions in HKUST-1 and their influence on framework degradation. Previous theoretical calculations have focused on adsorption energies of ammonia and water to Cu^{2+} and thermal degradation of HKUST-1. For example, Watanabe et al. have calculated the binding energy of different molecules such as NO, H_2O, NH_3, CO, C_2H_2, and H_2S and found that pyridine and ammonia have the highest binding energy. Adsorption of ammonia was observed to cause a ~ 4.2% volume contraction of the structure and a decrease in the Cu–O bond by ~1.9%. Even though a pair of ammonia molecules adsorbed at the metal center has a higher binding energy than water, it was found that a significant amount of water binds due to the large water chemical potential at high partial pressures (10^{-3}–10^{-2} Torr).[42] Huang et al. reported molecular dynamic simulations of the framework thermal stability and found that HKUST-1 structure is stable up to 565 K. Above 800 K decomposition of HKUST-1 was observed to produce CO, O_2, CO_2, glassy carbon, and 1,3,5-benzenetricarboxylate.[46]

Implications of Ammonia–Water Cooperative Interactions. Results presented here for low loading conditions show that water residing in the pores may strengthen the ammonia–copper interactions compared to dry conditions. The stronger ammonia–copper interaction was observed to reduce the copper oxidation state (Cu^{2+} accepting one of the lone paired electrons (Figure 5)). Cu^{1+} usually forms lower coordination number compounds.[37,47] Moreover, hydrogen bonding of ammonia molecules at the higher loadings >1 NH_3:Cu^{2+} promotes hydrogen bonding and incorporation of water. Therefore, replacement of the linker by other molecules such as water is possible, leading to framework degradation at higher relative humidity and ammonia loadings previously observed by Peterson et al.[13]

4. CONCLUSIONS

NEXAFS and XPS measurements show that ammonia adsorbs at both Cu^{1+} and Cu^{2+} in HKUST-1. Adsorption on the Cu^{2+} unsaturated metal center weakens the metal–linker bond. The ammonia adsorbs to the Cu^{2+} through Lewis base interactions, while for Cu^{1+} the interaction is electrostatic in nature and is possible due to 4s and 3d orbital hybridization. For a hydrated film, ammonia replaces preadsorbed water at the unsaturated metal centers due to its higher binding energy. However, ~20% of the preadsorbed water remains in the pores due to hydrogen bonding between water and ammonia.

Evidence for cooperative interactions between hydrogen-bonded water to ammonia adsorbed at the Cu^{2+} are observed. These cooperative interactions result in the increased strength of the ammonia–Cu^{2+} interaction compared to ammonia adsorbed under dry conditions. Two situations exist depending on ammonia loading, one where water hydrogen bonds to a single ammonia molecule (low ammonia loading) and/or participation of two ammonia molecules and water in the hydrogen bond. Ammonia–ammonia hydrogen bonding is observed to enhance water co-adsorption. The presence of water in the pores and the cooperative effect, detected spectroscopically, can explain framework degradation observed in previous work occurring at higher pressures.[13,17]

■ ASSOCIATED CONTENT

Supporting Information

The Supporting Information is available free of charge on the ACS Publications website at DOI: 10.1021/acs.jpcc.5b05716.

DOI: 10.1021/acs.jpcc.5b05716
J. Phys. Chem. C 2015, 119, 24781–24788

X-ray diffraction of a 40 layer HKUST-1 film, Cu 2p photoelectron spectra, and Cu L3-edge spectra in the presence of only water, only ammonia, and both (PDF)

AUTHOR INFORMATION

Corresponding Author

*E-mail: nour.nijem@yahoo.com.

Author Contributions

The broad scope of the experiments was conceived by N.N., M.K.G., and S.R.L. Experiments were performed by N.N. and K.F. under the guidance of H.B., N.N. conceived of the specific experiments performed here and the data analysis (with guidance from H.B.) and wrote the manuscript. M.K.G., S.R.L, and H.B. all provided feedback and contributed to the manuscript preparation.

Notes

The authors declare no competing financial interest.

ACKNOWLEDGMENTS

M.K.G., H.B., and beamline 11.0.2 at the Advanced Light Source (ALS) are supported through the Condensed Phase and Interfacial Molecular Science Program of DOE. N.N. and S.R.L. were supported by the Office of the Secretary of Defense National Security Science and Engineering Faculty Fellowship. K.F. was supported by The German Academic Exchange Service (DAAD). The ALS is supported by the U.S. Department of Energy, Office of Science, Office of Basic Energy Sciences, Chemical Sciences, Geosciences and Biosciences Division at Lawrence Berkeley National Laboratory under Contract No. DE-AC02-05CH11231. The authors thank Dr. Martin Kunz and Dr. Kei Nakamura at the ALS micro diffraction facility on beamline 12.3.2.

REFERENCES

(1) Falcaro, P.; Ricco, R.; Doherty, C. M.; Liang, K.; Hill, A. J.; Styles, M. J. MOF positioning technology and device fabrication. *Chem. Soc. Rev.* **2014**, *43*, 5513−5560.

(2) Bradshaw, D.; Garai, A.; Huo, J. Metal−organic framework growth at functional interfaces: Thin films and composites for diverse applications. *Chem. Soc. Rev.* **2012**, *41*, 2344−2381.

(3) Isaeva, V. I.; Kustov, L. M. The application of metal−organic frameworks in catalysis (Review). *Pet. Chem.* **2010**, *50*, 167−180.

(4) Liu, J.; Chen, L.; Cui, H.; Zhang, J.; Zhang, L.; Su, C.-Y. Applications of metal−organic frameworks in heterogeneous supramolecular catalysis. *Chem. Soc. Rev.* **2014**, *43*, 6011−6061.

(5) Hu, Z.; Deibert, B. J.; Li, J. Luminescent metal−organic frameworks for chemical sensing and explosive detection. *Chem. Soc. Rev.* **2014**, *43*, 5815−5840.

(6) Qiu, S.; Xue, M.; Zhu, G. Metal−organic framework membranes: From synthesis to separation application. *Chem. Soc. Rev.* **2014**, *43*, 6116−6140.

(7) Barea, E.; Montoro, C.; Navarro, J. A. R. Toxic gas removal—Metal−organic frameworks for the capture and degradation of toxic gases and vapours. *Chem. Soc. Rev.* **2014**, *43*, 5419−5430.

(8) Mason, J. A.; Veenstra, M.; Long, J. R. Evaluating metal−organic frameworks for natural gas storage. *Chem. Sci.* **2014**, *5*, 32−51.

(9) He, Y.; Zhou, W.; Qian, G.; Chen, B. Methane storage in metal−organic frameworks. *Chem. Soc. Rev.* **2014**, *43*, 5657−5678.

(10) Basdogan, Y.; Keskin, S. Simulation and modelling of MOFs for hydrogen storage. *CrystEngComm* **2015**, *17*, 261−275.

(11) Lu, W.; Wei, Z.; Gu, Z.-Y.; Liu, T.-F.; Park, J.; Park, J.; Tian, J.; Zhang, M.; Zhang, Q.; Gentle, T., III; Bosch, M.; Zhou, H.-C.; et al. Tuning the structure and function of metal−organic frameworks via linker design. *Chem. Soc. Rev.* **2014**, *43*, 5561−5593.

(12) Guillerm, V.; Kim, D.; Eubank, J. F.; Luebke, R.; Liu, X.; Adil, K.; Lah, M. S.; Eddaoudi, M. A supermolecular building approach for the design and construction of metal−organic frameworks. *Chem. Soc. Rev.* **2014**, *43*, 6141−6172.

(13) Peterson, G. W.; Wagner, G. W.; Balboa, A.; Mahle, J.; Sewell, T.; Karwacki, C. J. Ammonia vapor removal by $Cu_3(BTC)_2$ and its characterization by MAS NMR. *J. Phys. Chem. C* **2009**, *113*, 13906−13917.

(14) Petit, C.; Huang, L.; Jagiello, J.; Kenvin, J.; Gubbins, K. E.; Bandosz, T. J. Toward understanding reactive adsorption of ammonia on Cu-MOF/graphite oxide nanocomposites. *Langmuir* **2011**, *27*, 13043−13051.

(15) Petit, C.; Mendoza, B.; Bandosz, T. J. Reactive adsorption of ammonia on Cu-based MOF/graphene composites. *Langmuir* **2010**, *26*, 15302−15309.

(16) Petit, C.; Wrabetz, S.; Bandosz, T. J. Microcalorimetric insight into the analysis of the reactive adsorption of ammonia on Cu-MOF and its composite with graphite oxide. *J. Mater. Chem.* **2012**, *22*, 21443−21447.

(17) Borfecchia, E.; Maurelli, S.; Gianolio, D.; Groppo, E.; Chiesa, M.; Bonino, F.; Lamberti, C. Insights into adsorption of NH_3 on HKUST-1 metal−organic framework: A multitechnique approach. *J. Phys. Chem. C* **2012**, *116*, 19839−19850.

(18) Nijem, N.; Bluhm, H.; Ng, M. L.; Kunz, M.; Leone, S. R.; Gilles, M. K. Cu^{1+} in HKUST-1: Selective gas adsorption in the presence of water. *Chem. Commun.* **2014**, *50*, 10144.

(19) Nijem, N.; Chabal, Y. J. Adsorbate interactions in metal organic frameworks studied by vibrational spectroscopy. *Comments Inorg. Chem.* **2014**, *34*, 78−102.

(20) Nijem, N.; Kong, L.; Zhao, Y.; Wu, H.; Li, J.; Langreth, D. C.; Chabal, Y. J. Spectroscopic evidence for the influence of the benzene sites on tightly bound H_2 in metal organic frameworks with unsaturated metal centers: MOF-74-cobalt. *J. Am. Chem. Soc.* **2011**, *133*, 4782−4784.

(21) Nijem, N.; Thissen, P.; Yao, Y.; Longo, R. C.; Roodenko, K.; Wu, H.; Zhao, Y.; Cho, K.; Li, J.; Langreth, D. C.; et al. Understanding the preferential adsorption of CO_2 over N_2 in a flexible metal organic framework. *J. Am. Chem. Soc.* **2011**, *133*, 12849−12857.

(22) Nijem, N.; Veyan, J.-F.; Kong, L.; Li, K.; Pramanik, S.; Zhao, Y.; Li, J.; Langreth, D.; Chabal, Y. J. Interaction of molecular hydrogen with microporous metal organic framework materials at room temperature. *J. Am. Chem. Soc.* **2010**, *132*, 1654−1664.

(23) Nijem, N.; Veyan, J. F.; Kong, L.; Wu, H.; Zhao, Y.; Li, J.; Langreth, D. C.; Chabal, Y. J. Molecular hydrogen "pairing" interaction in a metal organic framework system with unsaturated metal centers (MOF-74). *J. Am. Chem. Soc.* **2010**, *132*, 14834−14848.

(24) Nijem, N.; Wu, H.; Canepa, P.; Marti, A.; Balkus, K. J.; Thonhauser, T.; Li, J.; Chabal, Y. J. Tuning the gate opening pressure of metal−organic frameworks (MOFs) for the selective separation of hydrocarbons. *J. Am. Chem. Soc.* **2012**, *134*, 15201−15204.

(25) Stavila, V.; Volponi, J.; Katzenmeyer, A. M.; Dixon, M. C.; Allendorf, M. D. Kinetics and mechanism of metal−organic framework thin film growth: Systematic investigation of HKUST-1 deposition on QCM electrodes. *Chem. Sci.* **2012**, *3*, 1531−1540.

(26) Liu, B.; Ma, M.; Zacher, D.; Bétard, A.; Yusenko, K.; Metzler-Nolte, N.; Wöll, C.; Fischer, R. A. Chemistry of SURMOFs: Layer-selective installation of functional groups and post-synthetic covalent modification probed by fluorescence microscopy. *J. Am. Chem. Soc.* **2011**, *133*, 1734−1737.

(27) Nijem, N.; Fürsich, K.; Kelly, S. T.; Swain, C.; Leone, S. R.; Gilles, M. K. HKUST-1 thin film layer-by-layer liquid phase epitaxial growth: Film properties and stability dependence on layer number. *Cryst. Growth Des.* **2015**, *15*, 2948−2957.

(28) Ogletree, F. D.; Bluhm, H.; Hebenstreit, E. D.; Salmeron, M. Photoelectron spectroscopy under ambient pressure and temperature conditions. *Nucl. Instrum. Methods Phys. Res., Sect. A* **2009**, *601*, 151−160.

(29) Bluhm, H.; Andersson, K.; Araki, T.; Benzerara, K.; Brown, G. E.; Dynes, J. J.; Ghosal, S.; Gilles, M. K.; Hansen, H. C.; Hemminger, J.

DOI: 10.1021/acs.jpcc.5b05716
J. Phys. Chem. C 2015, 119, 24781−24788

C.; et al. Soft X-ray microscopy and spectroscopy at the molecular environmental science beamline at the Advanced Light Source. *J. Electron Spectrosc. Relat. Phenom.* **2006**, *150*, 86−104.
(30) Yeh, J. J.; Lindau, I. Atomic subshell photoionization cross sections and asymmetry parameters: $1 \leq Z \leq 103$. *At. Data Nucl. Data Tables* **1985**, *32*, 1−155.
(31) Schlichte, K.; Kratzke, T.; Kaskel, S. Improved synthesis, thermal stability and catalytic properties of the metal−organic framework compound $Cu_3(BTC)_2$. *Microporous Mesoporous Mater.* **2004**, *73*, 81−88.
(32) Nijem, N.; Canepa, P.; Kong, L.; Wu, H.; Li, J.; Thonhauser, T.; Chabal, Y. J. Spectroscopic characterization of van der Waals interactions in a metal organic framework with unsaturated metal centers: MOF-74−Mg. *J. Phys.: Condens. Matter* **2012**, *24*, 424203.
(33) Canepa, P.; Nijem, N.; Chabal, Y. J.; Thonhauser, T. Diffusion of small molecules in metal organic framework materials. *Phys. Rev. Lett.* **2013**, *110*, 026102.
(34) George, S. J.; Lowery, M. D.; Solomon, E. I.; Cramer, S. P. Copper L-edge spectral studies: A direct experimental probe of the ground-state covalency in the blue copper site in plastocyanin. *J. Am. Chem. Soc.* **1993**, *115*, 2968−2969.
(35) Tjeng, L. H.; Chen, C. T.; Ghijsen, J.; Rudolf, P.; Sette, F. Giant Cu 2p resonances in CuO valence-band photoemission. *Phys. Rev. Lett.* **1991**, *67*, 501−504.
(36) St. Petkov, P.; Vayssilov, G. N.; Liu, J.; Shekhah, O.; Wang, Y.; Wöll, C.; Heine, T. Defects in MOFs: A thorough characterization. *ChemPhysChem* **2012**, *13*, 2025−2029.
(37) Fang, Z.; Dürholt, J. P.; Kauer, M.; Zhang, W.; Lochenie, C.; Jee, B.; Albada, B.; Metzler-Nolte, N.; Pöppl, A.; Weber, B.; et al. Structural complexity in metal−organic frameworks: Simultaneous modification of open metal sites and hierarchical porosity by systematic doping with defective linkers. *J. Am. Chem. Soc.* **2014**, *136*, 9627−9636.
(38) Shimizu, K.-i.; Maeshima, H.; Yoshida, H.; Satsuma, A.; Hattori, T. Ligand field effect on the chemical shift in XANES spectra of Cu(II) compounds. *Phys. Chem. Chem. Phys.* **2001**, *3*, 862−866.
(39) Inoue, K.; Ohashi, K.; Iino, T.; Judai, K.; Nishi, N.; Sekiya, H. Coordination and solvation of copper ion: Infrared photodissociation spectroscopy of $Cu^+(NH_3)_n$ (n = 3−8). *Phys. Chem. Chem. Phys.* **2007**, *9*, 4793−4802.
(40) McMillen, J. H. Elastic electron scattering in gases. *Rev. Mod. Phys.* **1939**, *11*, 84−110.
(41) Kerber, S. J.; Bruckner, J. J.; Wozniak, K.; Seal, S.; Hardcastle, S.; Barr, T. L. The nature of hydrogen in X-ray photoelectron spectroscopy: General patterns from hydroxides to hydrogen bonding. *J. Vac. Sci. Technol., A* **1996**, *14*, 1314−1320.
(42) Watanabe, T.; Sholl, D. S. Molecular chemisorption on open metal sites in Cu_3(benzenetricarboxylate)$_2$: A spatially periodic density functional theory study. *J. Chem. Phys.* **2010**, *133*, 094509.
(43) Hodgson, A.; Haq, S. Water adsorption and the wetting of metal surfaces. *Surf. Sci. Rep.* **2009**, *64*, 381−451.
(44) Schiros, T.; Ogasawara, H.; Näslund, L. Å.; Andersson, K. J.; Ren, J.; Meng, S.; Karlberg, G. S.; Odelius, M.; Nilsson, A.; Pettersson, L. G. M. Cooperativity in surface bonding and hydrogen bonding of water and hydroxyl at metal surfaces. *J. Phys. Chem. C* **2010**, *114*, 10240−10248.
(45) Van Humbeck, J. F.; McDonald, T. M.; Jing, X.; Wiers, B. M.; Zhu, G.; Long, J. R. Ammonia capture in porous organic polymers densely functionalized with brønsted acid groups. *J. Am. Chem. Soc.* **2014**, *136*, 2432−2440.
(46) Huang, L.; Joshi, K. L.; Duin, A. C. T. v.; Bandosz, T. J.; Gubbins, K. E. ReaxFF molecular dynamics simulation of thermal stability of a $Cu_3(BTC)_2$ metal−organic framework. *Phys. Chem. Chem. Phys.* **2012**, *14*, 11327−11332.
(47) Gaudin, E.; Boucher, F.; Evain, M. Some factors governing Ag^+ and Cu^+ low coordination in chalcogenide environments. *J. Solid State Chem.* **2001**, *160*, 212−221.

DOI: 10.1021/acs.jpcc.5b05716
J. Phys. Chem. C 2015, 119, 24781−24788